

TITLE:

**SPHINGOSINE 1-PHOSPHATE MEDIATES ADIPONECTIN RECEPTOR
SIGNALING ESSENTIAL FOR LIPID HOMEOSTASIS AND EMBRYOGENESIS**

RUNNING TITTLE: S1P promotes membrane homeostasis

AUTHORS: Mario Ruiz^{1*}, Ranjan Devkota¹, Dimitra Panagaki¹, Per-Olof Bergh², Delaney Kaper¹, Marcus Henricsson², Ali Nik¹, Kasparas Petkevicius³, Johanna L. Höög¹, Mohammad Bohlooly-Y³, Peter Carlsson¹, Jan Borén², Marc Pilon^{1*}

AFFILIATIONS:

¹Dept. Chemistry and Molecular Biology, Univ. Gothenburg, 405 30 Gothenburg, Sweden,

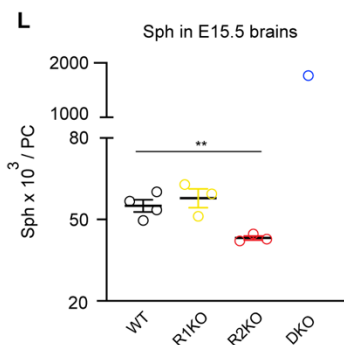
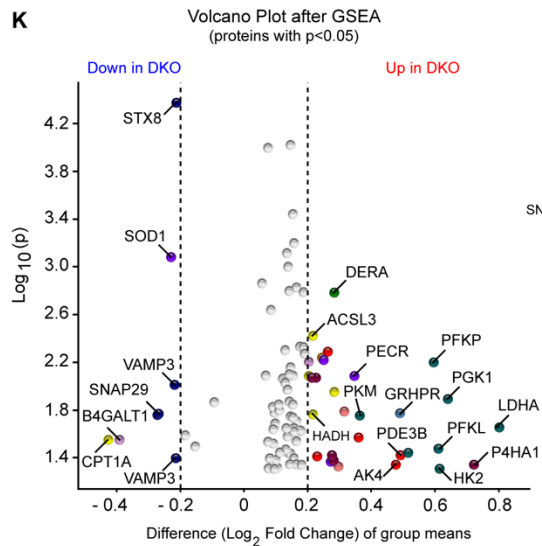
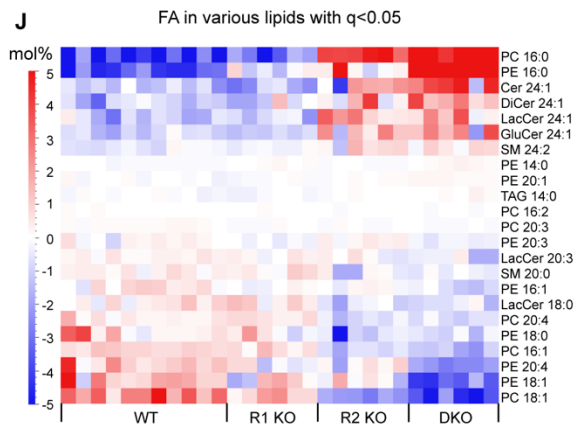
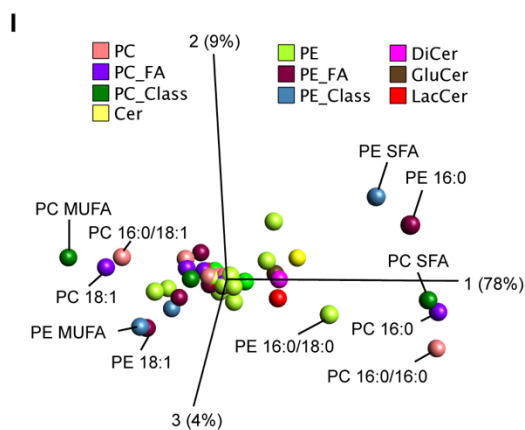
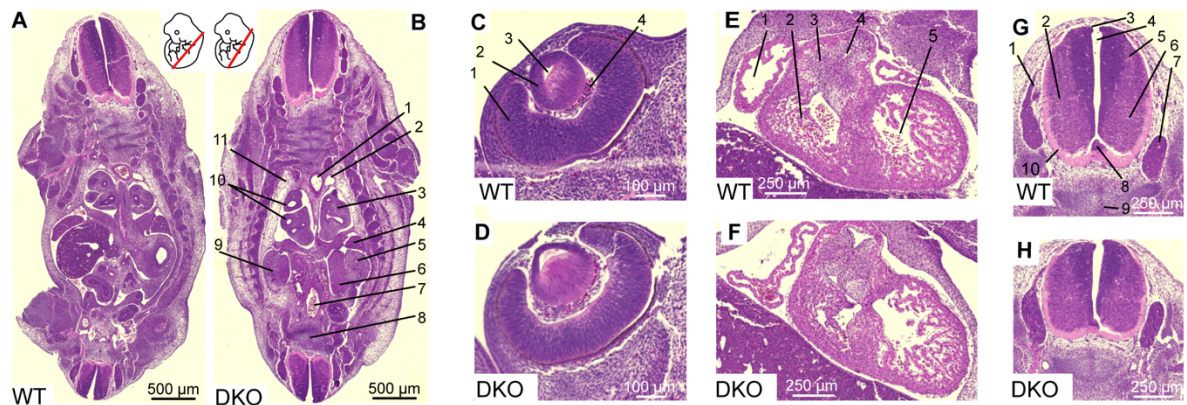
²Dept. Molecular and Clinical Medicine/Wallenberg Laboratory, Institute of Medicine, Univ. of Gothenburg, 414 67 Gothenburg, Sweden,

³Discovery Biology, Discovery Sciences, R&D, AstraZeneca, Gothenburg, Sweden.

CORRESPONDING TO: * Mario Ruiz (mario.ruiz.garcia@gu.se) or Marc Pilon (marc.pilon@cmb.gu.se), Dept. Chem Mol Biol, Univ. Gothenburg, Box 462, Gothenburg, SE-405 30, Sweden. Tel: +46 31 786 4952.

Supplementary Information

- Supplementary Fig. 1-8
- Supplementary Table 1-2
- Supplementary References
- Uncropped Blot S6D



Supplementary Fig.1 Membrane Lipid Composition Defects Precede Embryonic Lethality in DKO Mice (related to Fig.1).

(A-H) Sections of WT and DKO embryos at E12.5 stained with H&E. In C: 1. thoracic (descending) aorta; 2. left subcardinal vein; 3. segmental bronchus (left lung); 4. left lobe of liver; 5. left metanephros (kidney); 6. rete ovarii (early stage of differentiation); 7. sacral vein; 8. notochord; 9. right metanephros (kidney); 10. segmental bronchus (right lung); 11. loose connective tissue forming wall of pericardio-peritoneal cavity. In D: 1. inner (neural) layer of retina; 2. lens; 3. lens vesicle; 4. hyaloid cavity. In F: 1. right atrium; 2. right ventricle; 3. leaflets of pulmonary valve; 4. origin of pulmonary trunk; 5. left ventricle. In H: 1. dorsal nerve root; 2. mantle; 3. roof plate; 4. central canal; 5. alar plate; 6. basal plate; 7. dorsal root ganglion; 8. floor plate; 9. notochord; 10. marginal zone. Three embryos of each genotype were examined with similar results.

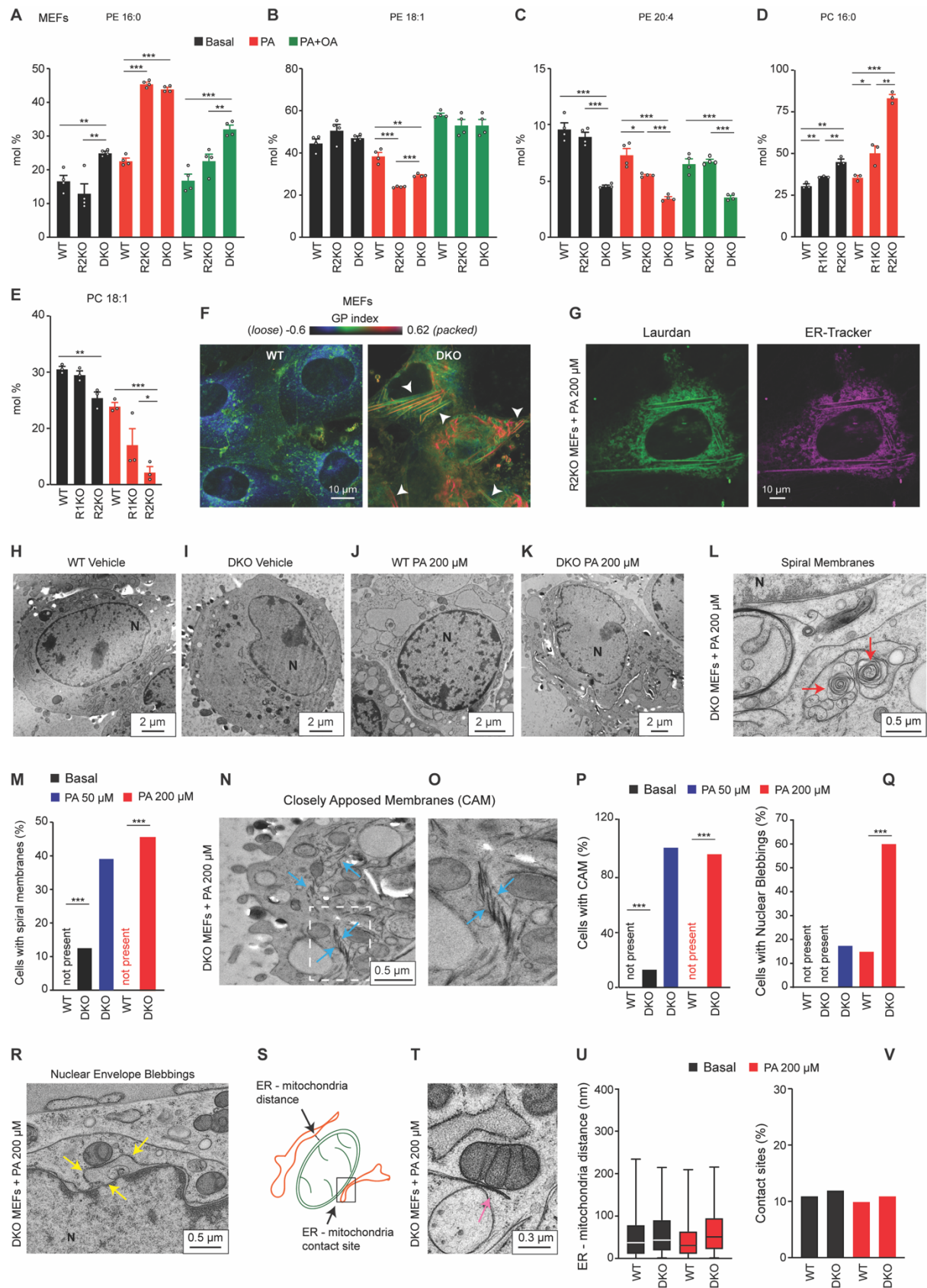
(I) PCA showing the variables responsible for the genotype separation in Fig.1D.

(J) Heatmap of all the lipid species with a $q < 0.05$ when comparing WT, R1KO, R2KO, DKO embryos at E12.5. Variables considered as in panel D. Note that WT embryos were enriched in PC with 16:1 and PE with 18:1 (both MUFA) whereas DKO had elevated PC with 16:0 and PE with 16:0 (SFA). Related lipidomics are included in Supplementary Data 2.

(K) Volcano plot of the proteomics showing all significant proteins after GSEA (97 in total), between WT and DKO at E12.5. Note that only the proteins with a \log_2 difference $>$ than 0.2 from WT and with a $p < 0.05$ are colored and labeled. See Supplementary Data 3 for the full list.

(L) Sph abundance in mouse embryonal brains at E15.5. $n=4$, 3, 3 and 1 biologically independent replicate for WT, R1KO, R2KO and DKO, respectively. Error bars show the standard error of the mean, and t-tests (two sided and assuming normality) were used to identify significant differences. Related lipidomics are shown Supplementary Data S2.

See also Supplementary Data 1-3. Data are represented as mean \pm SEM. $**p < 0.01$. Source data are provided as a Source Data file.



Supplementary Fig.2 S1P Rescues Membrane Homeostasis Defects Caused by the Absence of AdipoR2 in MEFs (related to Fig.2).

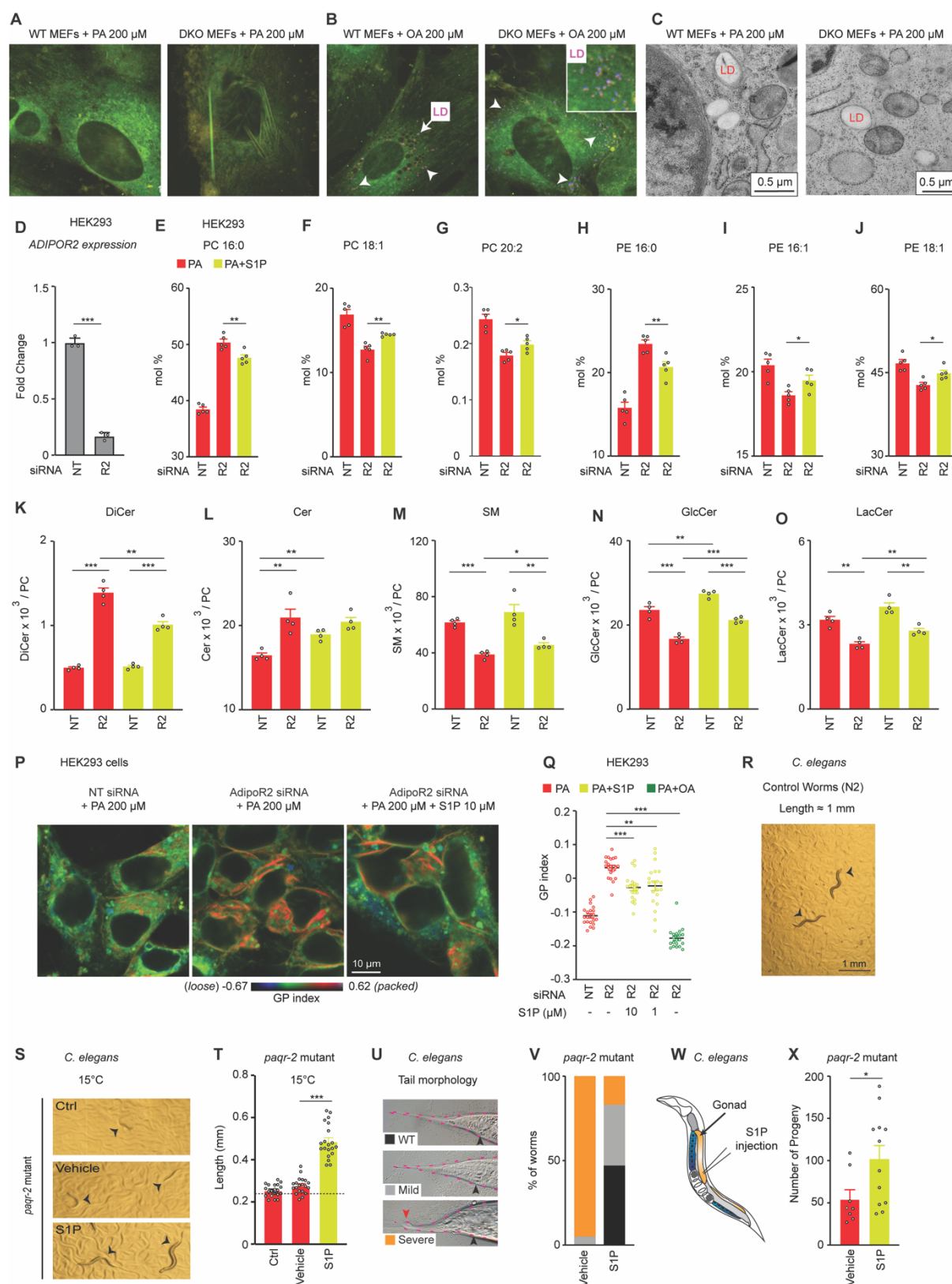
(A-E) PA (16:0), OA (18:1) and AA (20:4) abundance (mol%) in the PC and/or PE of WT, R1KO R2KO and DKO MEFs cultivated in the presence of vehicle, PA 200 μ M \pm OA 200 μ M for 18 h. For A-C, n=4 independent biological replicates per condition. For D-E, n=3 independent biological replicates per condition. Related lipidomics are shown in Supplementary Data 4.

(F) Pseudocolor images of WT and DKO MEFs challenged with PA 200 μ M and stained with Laurdan. Note that pixels with highly packed lipids are colored in red and appear only in DKO MEFs. White arrows indicate long and packed structures exclusively present in DKO cells. **(G)** Single channel confocal images of live R2KO MEFs stained with Laurdan (left picture) and ER-Tracker (right picture). Merged image is shown in Fig.2I.

(H-K) Electron microscopy pictures with a general cellular view of WT and DKO MEFs exposed to vehicle (F-G) and PA 200 μ M (H-I).

(L-M) DKO MEFs images showing distinct spiral membranes (marked by red arrows) in the cytoplasm and the quantification. For each condition from left to right, n=27, 27, 24, 23 and 22. N in the pictures indicates the nucleus. **(N-P)** Representative image (and zoom in) of DKO MEFs exposed to PA 200 μ M and showing electron dense closely apposed membranes (CAM, labeled with blue arrows) and the quantification (n=22-27 sections). The white square in N indicates the region magnified in O. **(Q-R)** Representative image of DKO MEFs treated with PA 200 μ M and showing nuclear envelop blebbing (yellow arrows) and the quantification (n=17-27 sections). N in the pictures indicates the nuclei.

(S-V) Cartoon, representative EM image and quantification of ER-mitochondria distance (n \approx 100) and contact-sites in WT or DKO MEFs in basal media and treated with PA 200 μ M. Error bars show the standard error of the mean, except for U where the boxes indicate the 25th to 75th percentile while the whiskers indicate the data points still within 1.5 of the box range. t-tests (two sided and assuming normality) were used to identify significant differences between treatments. *p<0.05, **p<0.01, ***p<0.001. See also Supplementary Data 4. Source data are provided as a Source Data file.



Supplementary Fig.3 Loss of AdipoRs Causes Multiple Membrane Defects in MEFs, HEK293 Cells and in *C. elegans* (related to Fig.2).

(A-B) Representative images of MEFs stained with Laurdan (green and red color) and LipidSpot 610 (purple dots pointed by white arrows).

(C) Representative EM images of MEFs.

(D) qPCR showing the efficiency of the AdipoR2 knockdown in HEK293 cells. n=3 technical replicate per condition.

(E-J) PA 16:0), OA (18:1) and eicosadienoic (20:2n-6) fatty acid abundance (mol%) in the PC and PA, PalOA (16:1) and OA in the PE of HEK293 cells cultivated in the presence of PA 200 μ M \pm S1P 1 μ M and treated with NT and AdipoR2 siRNA. n=5 independent biological replicates per condition. Related Lipidomics are shown in Supplementary Data 6.

(K-O) DiCer, Cer, SM, GlcCer and LacCer in HEK293 cells cultivated in the presence of PA 200 μ M \pm S1P 1 μ M and treated with NT or AdipoR2 siRNA. n=4 independent biological replicates per condition. From Supplementary Data 6.

(P-Q) Pseudocolor images and GP index of HEK293 cells treated with PA 200 μ M \pm S1P (10 and 1 μ M) or \pm OA 200 μ M and stained with Laurdan dye.

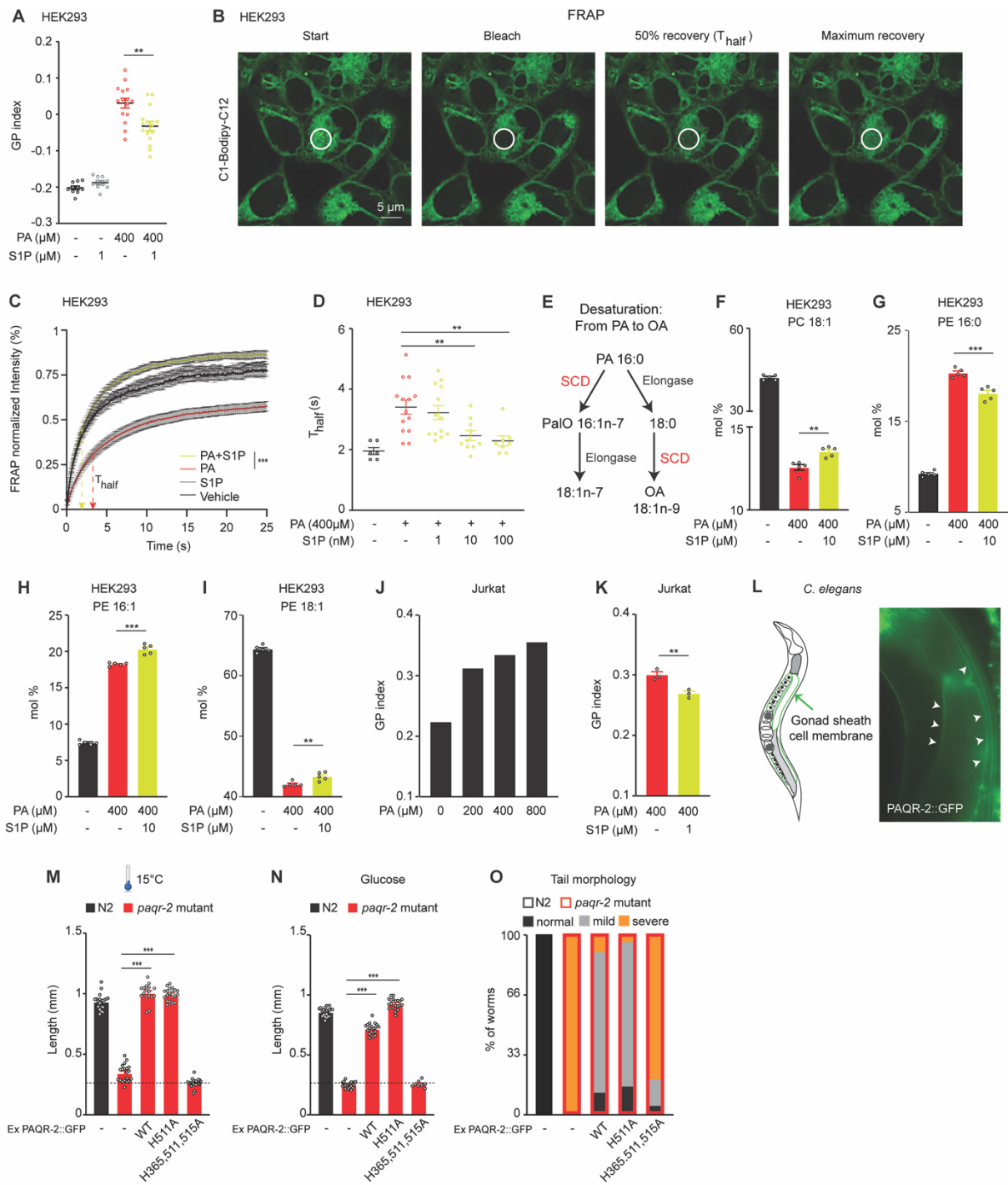
(R) Representative picture of WT 1-day adult *C. elegans*.

(S-T) Representative pictures and quantification of the length of *paqr-2* mutant worms (arrowheads) grown on control plates or vehicle \pm S1P 25 μ M at 15°C for 144 h. The dashed line in S represents the approximate length of the L1s at the start of the experiments. n= 20 worms measured per condition.

(U-V) Representative images and quantification (n=50 worms/genotype) of the tail tip morphology of 1-day adult *C. elegans*: WT phenotype, and mild and severe defects are shown. Shorter and broader tail tips were scored as mild defect, whereas deformed and bumpy tails were scored as severe defect (indicated by the red arrow). Black arrows indicate the anus.

(W-X) Schematic representation of *C. elegans*. The region of the gonad where S1P was injected is highlighted in orange. Brood size of *paqr-2* mutant injected with vehicle \pm S1P 10 μ M. n=8 and 12 independently injected worms for vehicle the S1P treatment, respectively.

Data are means \pm SEM, except in D: \pm SD. t-tests (two sided and assuming normality) were used to identify significant differences between treatments. *p<0.05, **p<0.01, ***p<0.001. See also Supplementary Data 6. Source data are provided as a Source Data file.



Supplementary Fig.4. S1P Promotes Membrane Homeostasis in Multiple Human Cell Types and in *C. elegans* (related to Fig.3).

(A) Average GP index from several images of HEK293 cells treated as indicated. For each condition, from left to right, n=10, 10, 15 and 15 separate images analyzed.

(B-D) C1-Bodipy-C12 staining of live HEK293 cells indicating different phases during a FRAP experiment (start, bleach, 50% recovery and end). The white circle represents the FRAP region. Panel C shows the normalized fluorescence intensity during the FRAP experiment of cells treated with vehicle, S1P 1 μ M, and PA 400 μ M \pm S1P 1 μ M. Panel D shows the average Thalf values from the curves in C. In D, for each condition, from left to right, n=6, 14, 13, 10 and 7 separate images analyzed.

(E) Pathway showing how PA (16:0) is desaturated (and elongated) to become 18:1.

(F-I) PalO (16:1) and OA (18:1) abundance (mol%) in the PC and PE of HEK293 cells treated as indicated. In G-I, n=5 independent biological replicates per condition. Data from Supplementary Data S5.

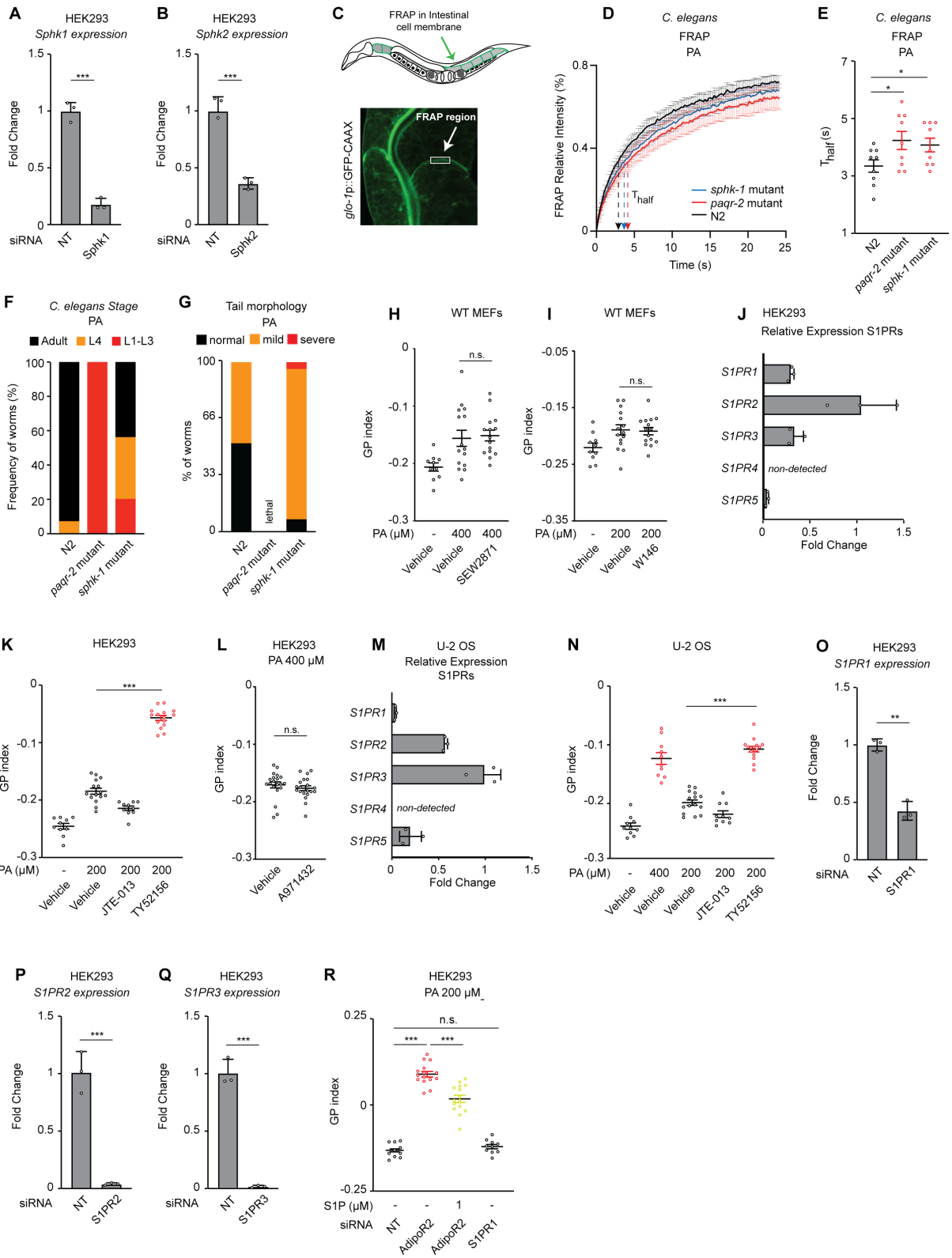
(J-K) Average GP index from cytometry experiments of Jurkat E6.1 cells treated with PA (panel J) or with PA 400 μ M \pm S1P (panel K) for 18 h and stained with Laurdan. In J, n=1 and K, n=3 independent biological replicates analyzed by flow cytometry.

(L) Representation of *C. elegans* highlighting the gonad sheath cell membrane in green (tissue were PAQR-2::GFP is easily visualized) and a fluorescent picture of the actual gonad sheath cell membrane (white arrows).

(M-N) Length of N2 and *paqr-2* mutant worms expressing PAQR-2::GFP with WT sequence or with H511A and H365,511,516A variants. Worms were grown at 15°C for 144 h (panel M) or at 20°C on glucose plates for 72 h (panel N). Note that glucose is readily converted to SFAs by the dietary *E. coli* (Devkota et al., 2017). The dashed line represents the approximate length of the L1s at the start of the experiments. In M, from left to right, n= 20, 20, 15, 20 and 20 worms measured per condition. In N, from left to right, n=20, 19, 19, 20 and 8 worms measured per condition.

(O) Quantification of the tail tip morphology of 1-day adult N2 and *paqr-2* mutant worms expressing different PAQR-2::GFP variants (n=50 worms/genotype DK). Examples of the different tail morphologies are shown in Supplementary Fig.3U.

Data are means \pm SEM, and t-tests (two sided and assuming normality) were used to identify significant differences between treatments. Data shows mean \pm SEM. *p<0.05, **p<0.01, ***p<0.001. See also Supplementary Data 5-S6. Source data are provided as a Source Data file.



Supplementary Fig.5 Sphingosine Kinases and S1PR3 Are Required to Maintain Membrane Homeostasis in Mammalian Cells and *C. elegans* (related to Fig.4)

(A-B) qPCR showing the efficiencies of the Sphk1 and Sphk2 knockdowns. n=3 technical replicate per condition.

(C) Schematic representation of *C. elegans* (note that the membrane of intestinal cells is decorated in green representing a membrane-bound prenylated GFP) and a confocal image of the actual GFP signal in intestinal cells of *C. elegans*. The white square represents the FRAP region.

(D-E) Curves and T_{half} values of the normalized fluorescence during a FRAP experiment of worms grown in PA 2 mM plates. In E, n=9 worms scored for each genotype.

(F-G) Quantification of *C. elegans* larval stages and adulthood after 72 h growing at 20°C in F, and tail tip morphology of 1-day adult worms grown on plates with PA-loaded OP50 bacteria in G (n=50 worms/genotype). Examples of the different tail morphologies are shown in Supplementary Fig.3U.

(H-I) Average GP index from several images of WT MEFs treated with vehicle, PA 400 μ M \pm SEW2871 1 μ M (S1PR1 agonist) in H and PA 400 μ M \pm W146 5 μ M (S1PR1 antagonist) in I. In H, for each condition from left to right, n=10, 15 and 15 separate images analyzed. In I, for each condition from left to right, n=10, 15 and 15 separate images analyzed.

(J) Relative expression of S1PRs in HEK293 cells measured by qPCR. n=3 technical replicate per condition.

(K-L) Average GP index from several images of HEK293 cells treated with vehicle, PA 200 μ M \pm JTE-013 5 μ M (S1PR2 antagonist), \pm TY52156 5 μ M (S1PR3 antagonist) in K and PA 400 μ M \pm A971432 1 μ M (S1PR5 agonist) in L. In K, for each condition from left to right, n=10, 15, 10 and 15 separate images analyzed. In L, n=20 separate images analyzed per condition.

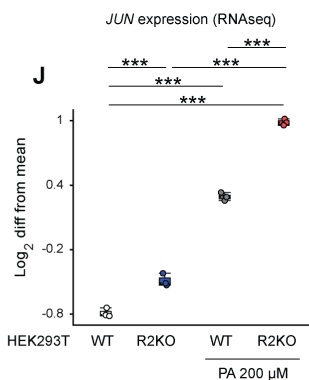
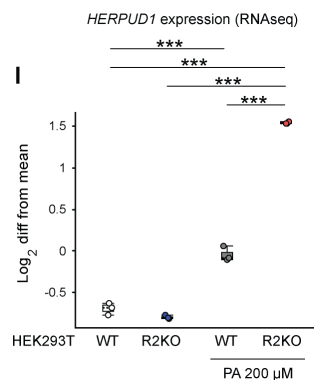
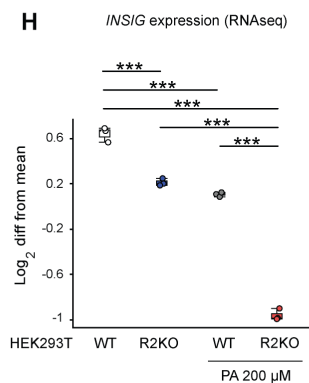
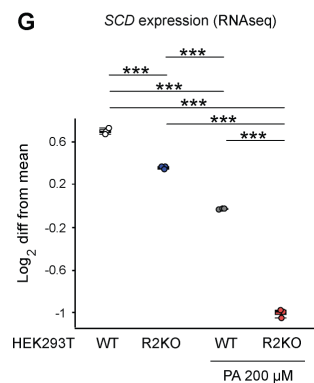
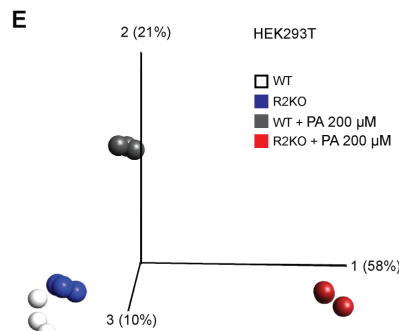
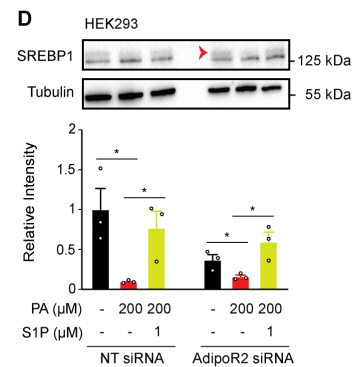
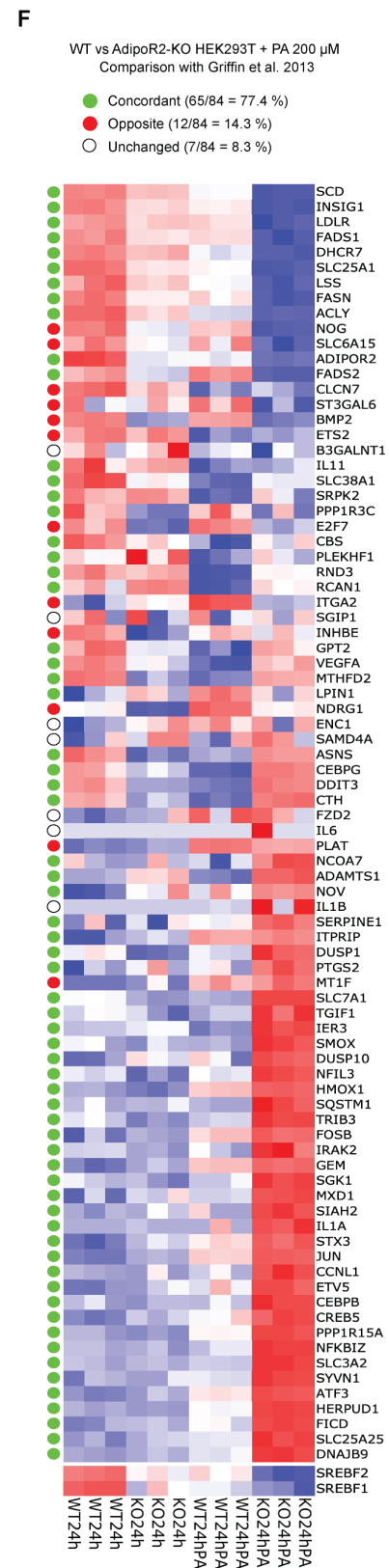
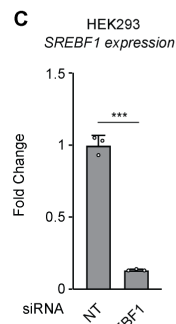
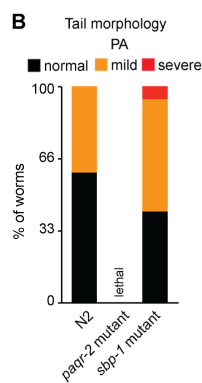
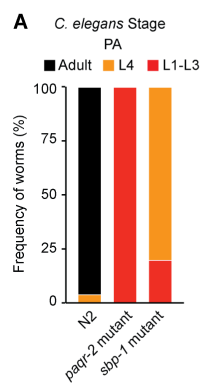
(M) Relative expression of S1PRs in U-2 OS cells measured by qPCR. n=3 technical replicate per condition.

(N) Average GP index from several images of U-2 OS cells treated with vehicle, PA 200 μ M \pm JTE-013 5 μ M (S1PR2 antagonist), \pm TY52156 5 μ M (S1PR3 antagonist). For each condition from left to right, n=10, 10, 15, 10 and 15 separate images analyzed.

(O-Q) qPCR showing the efficiencies of the S1PR1, S1PR2, S1PR3 knockdowns. n=3 technical replicate per condition.

(R) Average GP index from several images of NT, AdipoR2 and S1PR1 siRNA HEK293 cells treated with PA 200 μ M \pm S1P 1 μ M. For each condition from left to right, n=10, 15, 15 and 10 separate images analyzed.

Data shows mean \pm SEM in D-E, H-I, K-L, N and R and \pm SD in A-B, J, M and O-Q. t-tests (two sided and assuming normality) were used to identify significant differences between treatments. *p<0.05, **p<0.01, ***p<0.001. Source data are provided as a Source Data file.



Supplementary Fig.6. S1P Signaling Via SREBP1 Maintains Membrane Homeostasis in Human Cells and *C. elegans* (related to Fig.5).

(A-B) Quantification of *C. elegans* larval stages and adulthood in N2, *paqr-2* and *sbp-1* mutants after 72 h growing at 20°C in A and Tail tip morphology of 1-day adult worms grown on plates with PA-loaded OP50 bacteria in B (n=50 worms/genotype). Examples of the different tail morphologies are shown in Fig.S3U.

(C) qPCR result showing the efficiency of the SREBF1 siRNA knockdown by siRNA in HEK293 cells. n=3 technical replicate per condition.

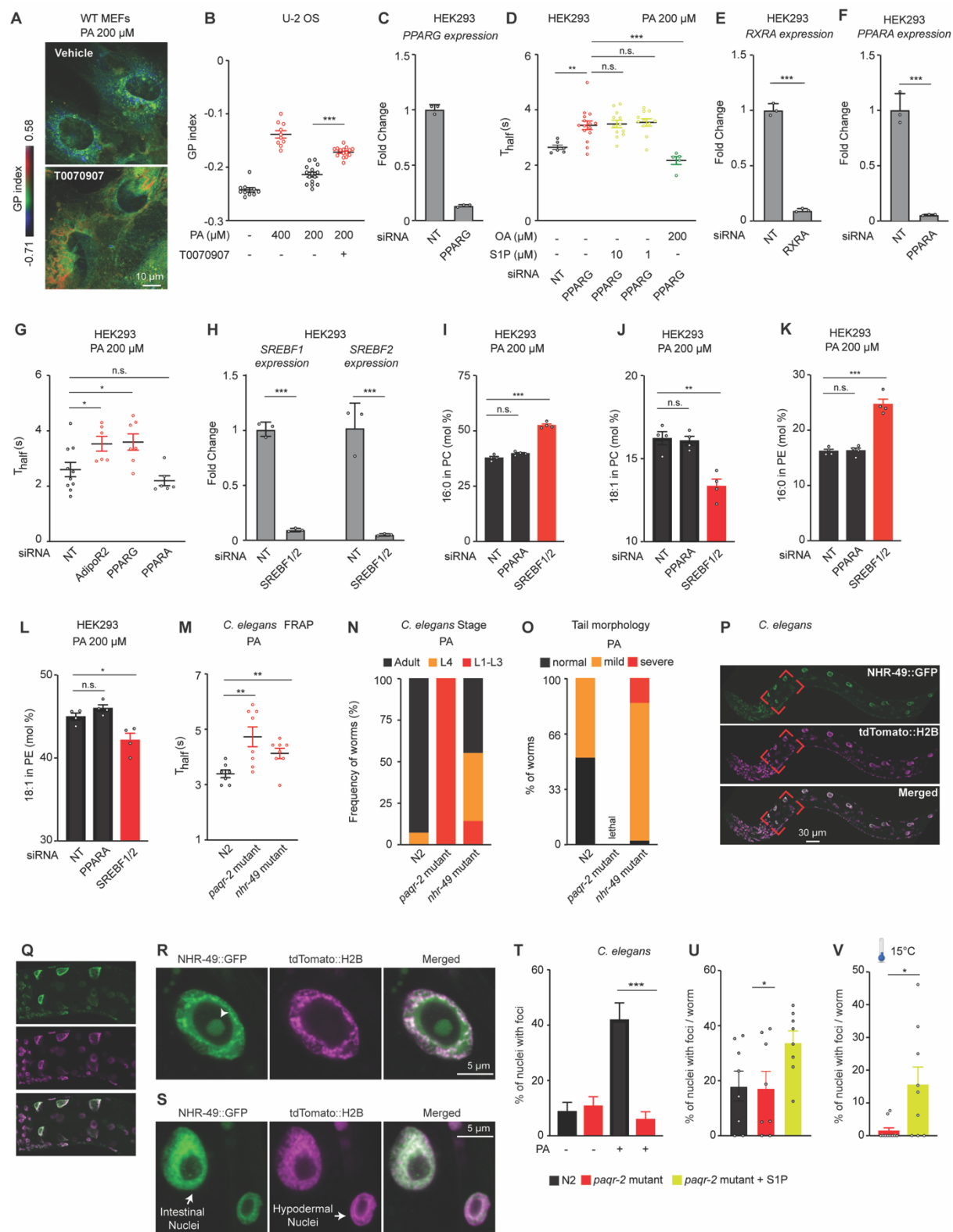
(D) Western-Blot and quantification (n=3 experiments) of NT and AdipoR2 siRNA HEK293 cells treated with vehicle and PA 200 μ M \pm S1P 1 μ M. The red arrow points to the precursor SREBP1 band. Note the presence of an unspecific band just below SREBP1. Uncropped blots in Source Data.

(E) PCA plot based on 84 SREBP-regulated genes from ¹ of WT or AdipoR2-KO HEK293T cells in basal media or basal media supplemented with PA 200 μ M for 24 h. Note that genotypes are well separated upon PA treatment.

(F) All 84 genes from ¹ listed in the order of the PC1, and labelled as to whether their changes in expression matched ¹. *SREBF1/2* were both downregulated in AdipoR2-KO cells and were added at the bottom of the heat map.

(G-J) Plots of four genes whose expression its highly altered by the loss of AdipoR2 or SREBP1/2. n=3 independent biological replicates per condition.

Data are represented as mean \pm SEM in D and \pm SD in C and G-J. t-tests (two sided and assuming normality) were used to identify significant differences between treatments. *p<0.05, ***p<0.001. See also Supplementary Data 5. Source data are provided as a Source Data file.



Supplementary Fig.7. S1P Signaling Via PPAR γ Maintains Membrane Homeostasis in Human/Mouse Cells and *C. elegans* (related to Fig.5).

(A) Pseudocolor images of WT MEFs treated with vehicle, PA 200 μ M \pm T0070907 1 μ M (PPAR γ antagonist). Quantification of several images is shown in Fig.5D.

(B) Average GP index of U-2 OS cells treated with vehicle, PA 400 μ M and PA 200 μ M \pm T0070907 1 μ M. For each condition from left to right, n=10, 10, 15 and 15 separate images analyzed.

(C) qPCR showing the efficiency of the PPARG knockdown. n=3 technical replicates per condition.

(D) FRAP experiment of NT and PPARG siRNA HEK293 cells treated with PA 200 μ M \pm S1P (10 or 1 μ M) and \pm OA 200 μ M. For each condition from left to right, n=6, 15, 12, 11 and 5 separate cells were analyzed.

(E) qPCR showing the efficiency of the RXRA knockdown. n=3 technical replicates per condition.

(F) qPCR showing the efficiency of the PPARA knockdown. n=3 technical replicates per condition.

(G) FRAP experiment in HEK293 cells. For each condition from left to right, n=10, 6, 15, 7 and 6 separate cells were analyzed.

(H) qPCR showing the efficiency of the SREBF1+2 knockdown. n=technical replicates per condition.

(I-L) PA 16:0) and OA (18:1) abundance (mol%) in the PC and in the PE of HEK293 cells cultivated as indicated. n=4 independent biological replicates per condition. From Supplementary Data S6.

(M) FRAP experiment on N2, *paqr-2* and *nhr-49* mutants fed PA-loaded OP50 bacteria. For each genotype from left to right, n=7, 8, and 8 separate worms analyzed.

(N-O) Quantification of *C. elegans* larval stages and adulthood in N2, *paqr-2* and *nhr-49* mutants after 72 h growing at 20°C in N. Tail tip morphology of 1-day adult worms grown on plates with PA-loaded OP50 bacteria in O (n=50 worms/genotype). Examples of the different tail morphologies are shown in Fig.S3U.

(P-S) Images of *C. elegans* expressing NHR-49::GFP and tdTomato::H2B (nuclear marker). Panels Q shows zoom-in of P. R shows higher magnification of an intestinal nucleus with nucleolar foci (arrowhead) while S shows intestinal and hypodermal nuclei.

(T-V) Quantification of the presence of nucleolar foci in intestinal nuclei of N2 and *paqr-2* mutants grown on control plates (S) and on plates supplemented with S1P at 20°C (T) and 15°C (V). In T, from left to right, n=59, 52, 53 and 43 worms scored. In U, n=8 worms scored. In V, n=10 for *paqr-2* mutant and n=9 for *paqr-2* mutant + S1P.

Data shows mean \pm SEM in B, D, G, I-L, S-U and \pm SD in C, E-F, H. t-tests (two sided and assuming normality) were used to identify significant differences between treatments. *p<0.05, **p<0.01, ***p<0.001. See also Supplementary Data 5-6. Source data are provided as a Source Data file.

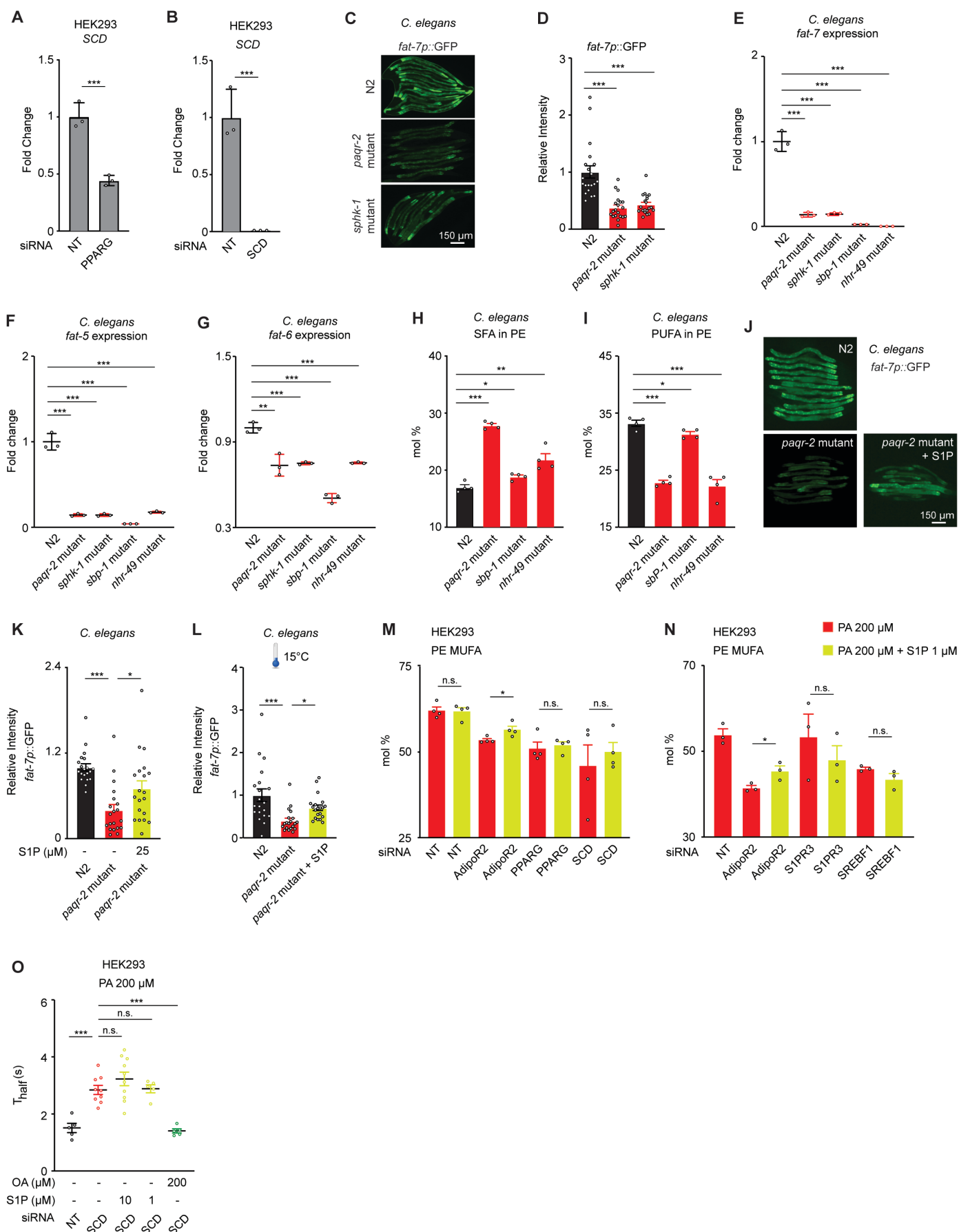


Figure S8. Role of SCD in Maintenance of Membrane Homeostasis in Human Cells and in *C. elegans* (related to Fig.6).

(A) Relative expression of *SCD* in NT and PPARG siRNA HEK293 cells measured by qPCR.

(B) qPCR result showing the efficiency of the SCD knockdown by siRNA in HEK293 cells n=3 technical replicates per condition.

(C-D) Representative images of *C. elegans* expressing GFP under the control of the *fat-7* promoter (*fat-7p::GFP*) and quantification of the fluorescence. N2 and *paqr-2* and *sphk-1* mutant worms were grown on control plates for 72 h.

(E-G) Relative expression of *fat-7*, *fat-5* and *fat-6* in N2, *paqr-2*, *sphk-1* and *nhr-49* mutant worms measured by qPCR.

(H-I) PA 16:0 and OA (18:1) abundance (mol%) and in the PE of *C. elegans* grown on PA 2 mM plates. Related lipidomics are shown in Supplementary Data 7.

(J-K) Representative images *C. elegans* expressing GFP under the control of the *fat-7* promoter (*fat-7p::GFP*) and the quantification of the fluorescence. N2 and *paqr-2* mutant worms were grown on control plates and plates supplemented with S1P 25 μ M for 72 h.

(L) Quantification of the fluorescence of *C. elegans* expressing GFP under the control of the *fat-7* promoter (*fat-7p::GFP*) grown at 15°C on control plates and plates supplemented with S1P 25 μ M for 144 h.

(M-N) MUFA abundance (mol%) and in the PE of HEK293 cells treated with different siRNA and PA 200 μ M \pm S1P 1 μ M. Related lipidomics are shown in Fig.6C-F and in Supplementary Data 6.

(O) FRAP experiment of NT and SCD siRNA HEK293 cells treated with PA 200 μ M \pm S1P (10 or 1 μ M) and \pm OA 200 μ M.

Data are represented as mean \pm SEM in D-I, K-O, I and \pm SD in A-B. t-tests (two sided and assuming normality) were used to identify significant differences between treatments.

*p<0.05, **p<0.01, ***p<0.001. See also Supplementary Data 5-7. Source data are provided as a Source Data file.

SUPPLEMENTARY TABLE 1

PCR PRIMERS

Primers used in this study (some primers were designed for previous studies).

| Sequence (5'-->3') | Organism | Purpose - Target | Reference |
|---|---------------------|--------------------------------------|------------|
| AGGCAGGGTAAGCTGATTAGCTATG TCCACTGTGTCAGCTTCTCTGTTAC GGGTGGGATTAGATAAATGCCTGCTCT | <i>Mus musculus</i> | Genotyping - <i>Adipor1</i> | 2 |
| GACGGAGTTTGTATGTGGTAGCGTC TCTCTGCCTTTCCTTTTCATGGCTC GGGCCAGCTCATTCTCCCACTCAT | <i>Mus musculus</i> | Genotyping / <i>Adipor2</i> | 2 |
| CTGCCTTTCACCTTGGAGAC CGTTTCCTGGGGATGAGATA | <i>Mus musculus</i> | qPCR - <i>Ddit3</i> | 3 |
| CATGGTTCTCACTAAAATGAAAGG GCTGGTACAGTAACAACCTG | <i>Mus musculus</i> | qPCR - <i>Hspa5</i> | 3 |
| ATGGCCGGCTATGGATGAT CGAAGTCAAACCTTTTCAGATCCATT | <i>Mus musculus</i> | qPCR - <i>Atf4</i> | 3 |
| GAGTCCGCAGCAGGTG TAAGACTCCTGCCTGACTGC | <i>Mus musculus</i> | qPCR - <i>sXBP1</i> | 4 |
| ACTACACAACGGGAGCAACAG GATGGAAAGCAGGAGCAGAG | <i>Mus musculus</i> | qPCR - <i>S1pr1</i> | 5 |
| CTCACTGCTCAATCCTGTCATC TTCACATTTTCCCTTCAGACC | <i>Mus musculus</i> | qPCR - <i>S1pr2</i> | 5 |
| TTCCCGACTGCTCTACCATC CCAACAGGCAATGAACACAC | <i>Mus musculus</i> | qPCR - <i>S1pr3</i> | 5 |
| TGCGGGTGGCTGAGAGTG TAGGATCAGGGCGAAGACC | <i>Mus musculus</i> | qPCR - <i>S1pr4</i> | 5 |
| CTTAGGACGCCTGGAAACC CCCGCACCTGACAGTAAATC | <i>Mus musculus</i> | qPCR - <i>S1pr5</i> | 5 |
| GTCTCCTTCGAGCTGTTTGC GCGTGTAAGTCACCAACCCT | <i>Mus musculus</i> | qPCR - <i>PPIA</i> (housekeeping) | This study |
| TGACCAACAAGGAGATGCGT AATTGTCCGATTTGCTGCGG | <i>Homo sapiens</i> | qPCR - <i>S1PR1</i> | This study |
| GCCTCTCTACGCCAAGCATT GCAGCCAGCAGACGATAAAG | <i>Homo sapiens</i> | qPCR - <i>S1PR2</i> | This study |
| TGAAGTCCAGCAGCCGTAAG AGCCAACACGATGAACCACT | <i>Homo sapiens</i> | qPCR - <i>S1PR3</i> | This study |
| CATCATGGGCCTCTATGGGG AGAGGTTGGAGCCAAAGACG | <i>Homo sapiens</i> | qPCR - <i>S1PR4</i> | This study |

| | | | |
|--|---------------------|--------------------------------------|------------|
| CTTTGTGGCATGTTGGGGC GCGTGTAGATGATGGGGTTCA | <i>Homo sapiens</i> | qPCR - <i>S1PR5</i> | This study |
| GACTGCCTGATTGACAAGCG ATTCTCGTTCCGGTCTTGCG | <i>Homo sapiens</i> | qPCR - <i>RXRA</i> | This study |
| ATGCTGGCTATGAGCAGGTC CCCAGACGCCGATACTTCTC | <i>Homo sapiens</i> | qPCR - <i>Sphk1</i> | This study |
| CCCCGGTTGCTTCTATTGGT GATCTAGGAGCCCCGTTTCAGC | <i>Homo sapiens</i> | qPCR - <i>Sphk2</i> | This study |
| GACCAAAGCAAAGGCGAGGG CAGCCCTGAAAGATGCGGATG | <i>Homo sapiens</i> | qPCR - <i>PPARG</i> | This study |
| GCGAACGATTGACTCAAGC TCGTCCAAAACGAATCGCGT | <i>Homo sapiens</i> | qPCR - <i>PPARA</i> | This study |
| GTCTCCTTTGAGCTGTTTGAG GGACAAGATGCCAGGACCC | <i>Homo sapiens</i> | qPCR - <i>PPIA</i> (housekeeping) | 6 |
| GACCTCGCAGATCCAGCAG ATAGGCAGCTTCTCCGCATC | <i>Homo sapiens</i> | qPCR - <i>SREBF1</i> | 7 |
| GTGCTGTTCTGACTCCCTG CAGCCTTCTTCTTGCCCTGA | <i>Homo sapiens</i> | qPCR - <i>SREBF2</i> | 7 |
| TTCGTTGCCACTTTCTTGCG TGGTGGTAGTTGTGGAAGCC | <i>Homo sapiens</i> | qPCR - <i>SCD</i> | 6 |
| CCATCTGCTTGGTTTCGTGC AGACGGTGTGAAAGAGCCAG | <i>Homo sapiens</i> | qPCR - <i>AdipoR1</i> | 6 |
| TCATCTGTGTGCTGGGCATT CTATCTGCCCTATGGTGGCG | <i>Homo sapiens</i> | qPCR - <i>AdipoR2</i> | 6 |
| TCTCGCAGGTTGTGTCTTCC AGCCTCATGGTAAGCCTTGT | <i>C. elegans</i> | qPCR - <i>tba-1</i> (housekeeping) | This study |
| CAGTTGGATGGGTATTCTCCT TCCATGAGAGGGTGGCTTTG | <i>C. elegans</i> | qPCR - <i>fat-5</i> | This study |
| GACCCAGTTCTCGTCTTCCA ATCCGAAATAGTGAGCAGCG | <i>C. elegans</i> | qPCR - <i>fat-6</i> | This study |
| GCCGTCTTCTCATTTGCTCTC ACGATGATCACGAGCCCAT | <i>C. elegans</i> | qPCR - <i>fat-7</i> | This study |

SUPPLEMENTARY TABLE 2

siRNA used in this study (some sequences were previously used by the authors).

| Target Gene | Catalog | Reference (Supplementary) |
|-------------|-------------|------------------------------|
| AdipoR2 | J-007801-10 | 6 |
| Non-Target | D-001810-10 | 6 |
| PPARA | J-003434-05 | - |
| PPARG | J-003436-08 | - |
| RXRA | J-003443-10 | - |
| S1PR1 | J-003655-06 | - |
| S1PR2 | J-003952-12 | - |
| S1PR3 | J-005208-06 | - |
| SCD | J-005061-07 | - |
| Sphk1 | J-004172-10 | - |
| Sphk2 | J-004831-10 | - |
| SREBF1 | J-006891-05 | 7 |
| SREBF2 | J-009549-05 | 7 |

SUPPLEMENTARY REFERENCES

1. Griffiths, B. *et al.* Sterol regulatory element binding protein-dependent regulation of lipid synthesis supports cell survival and tumor growth. *Cancer Metab* **1**, 3 (2013).
2. Bjursell, M. *et al.* Opposing effects of adiponectin receptors 1 and 2 on energy metabolism. *Diabetes* **56**, 583-593 (2007).
3. Rutkowski, D.T. *et al.* Adaptation to ER stress is mediated by differential stabilities of pro-survival and pro-apoptotic mRNAs and proteins. *PLoS Biol* **4**, e374 (2006).
4. Gomez, J.A. & Rutkowski, D.T. Experimental reconstitution of chronic ER stress in the liver reveals feedback suppression of BiP mRNA expression. *Elife* **5** (2016).
5. Zhang, L. *et al.* A novel role of sphingosine 1-phosphate receptor S1pr1 in mouse thrombopoiesis. *J Exp Med* **209**, 2165-2181 (2012).
6. Devkota, R. *et al.* The adiponectin receptor AdipoR2 and its *Caenorhabditis elegans* homolog PAQR-2 prevent membrane rigidification by exogenous saturated fatty acids. *PLoS Genet* **13**, e1007004 (2017).
7. Ruiz, M. *et al.* Extensive transcription mis-regulation and membrane defects in AdipoR2-deficient cells challenged with saturated fatty acids. *Biochim Biophys Acta Mol Cell Biol Lipids* **1866**, 158884 (2021).

